Chem. Senses 34: 349–358, 2009
doi:10.1093/chemse/bjp008
Advance Access publication March 20, 2009

# Role of Plasma Membrane Calcium ATPases in Calcium Clearance from Olfactory Sensory Neurons

**S. Ponissery Saidu[1], S.D. Weeraratne[2], M. Valentine[1], R. Delay[1] and Judith L. Van Houten[1]**

[1]Department of Biology and Vermont Chemosensory Group, University of Vermont, Burlington, VT 05405, USA and [2]Department of Neurology, Harvard Medical School, Children's Hospital, Boston, MA 02115, USA

*Correspondence to be sent to: Judith L. Van Houten, Department of Biology and Vermont Chemosensory Group, University of Vermont, Burlington, VT 05405, USA. e-mail: judith.vanhouten@uvm.edu*

## Abstract

Odorants cause $Ca^{2+}$ to rise in olfactory sensory neurons (OSNs) first within the ciliary compartment, then in the dendritic knob, and finally in the cell body. $Ca^{2+}$ not only excites but also produces negative feedback on the transduction pathway. To relieve this $Ca^{2+}$-dependent adaptation, $Ca^{2+}$ must be cleared from the cilia and dendritic knob by mechanisms that are not well understood. This work focuses on the roles of plasma membrane calcium pumps (PMCAs) through the use of inhibitors and mice missing 1 of the 4 PMCA isoforms (PMCA2). We demonstrate a significant contribution of PMCAs in addition to contributions of the $Na^+/Ca^{2+}$ exchanger and endoplasmic reticulum (ER) calcium pump to the rate of calcium clearance after OSN stimulation. PMCAs in neurons can shape the $Ca^{2+}$ signal. We discuss the contributions of the specific PMCA isoforms to the shape of the $Ca^{2+}$ transient that controls signaling and adaptation in OSNs.

**Key words:** calcium, kinetics, mouse, olfactory neurons, PMCA, pumps

## Introduction

Olfactory sensory neurons (OSNs) experience increases in intracellular calcium after odorants bind to G protein–coupled receptors on the cilia that protrude into the mucous covering of the olfactory epithelium. In response to the cyclic adenosine monophosphate (cAMP) produced when $G_{olf}$ activates adenylyl cyclase III (Bakalyar Reed 1990; Choi et al. 1992; Ronnett and Moon 2002), cyclic nucleotide–gated ion channels (CNGCs) open to allow an initial influx of $Ca^{2+}$ into the cilia. $Ca^{2+}$ subsequently rises in the dendritic knob and then in the dendrite and cell body (Leinders-Zufall et al. 1997). $Ca^{2+}$ enters the knob both through CNGCs (Firestein et al. 1991) and voltage-gated calcium channels that appear to be absent from the cilia (Leinders-Zufall et al. 1998; Bradley et al. 2001; Lagostena and Menini 2003; Gautam et al. 2007). $Ca^{2+}$ amplifies odor-evoked currents by activating $Cl^-$ channels that are responsible for the majority of the conductance (Kleene 1993). $Ca^{2+}$ also feeds back on the transduction system by inhibiting adenylyl cyclase (Leinders-Zufall et al. 1999) and CNGC (Kurahashi and Menini 1997; Bradley et al. 2001) as well as by activating a phosphodiesterase (Borisy et al. 1992) and $K^+$ channels. Whereas the mechanism of the $Ca^{2+}$ rise is well understood (Schild and Restrepo 1998), removal of $Ca^{2+}$, especially from the dendritic knob and cilia, is not well described. Clearance of calcium can depend upon multiple mechanisms including pumps, exchangers, and calcium-binding proteins, and the contribution of plasma membrane calcium pumps (PMCAs) to this process in OSNs is our focus.

PMCAs are more than mere cellular $Ca^{2+}$ "housekeepers." There are 4 PMCA isoforms and 25 favored splice variants with different tissue specificities, subcellular locations, and activities. PMCAs are regulated by the same intracellular messengers that play crucial roles in signal transduction in OSNs (Strehler et al. 2007). They are dynamic and even display a memory for the recent past (Caride, Penheiter, et al. 2001; Pottorf and Thayer 2002). The constellation of PMCA isoforms in a neuron determines the shape and duration of a transient calcium signal (Caride, Filoteo, et al. 2001). Thus, it matters whether the expressed isoform is 2 or 4, for example, or whether a splice variant is 4a rather than 4b, which differ in their activation and inactivation rates (Strehler et al. 2007). Therefore, elucidation of roles for PMCAs in OSN $Ca^{2+}$ clearance is more than an inventory of housekeeping enzymes.

Previously we demonstrated that all 4 PMCA isoforms are present in mouse OSNs and identified the splice variants (Weeraratne et al. 2006). Three isoforms (1, 2, and 4) are

found in the cilia and all 4 isoforms in the dendritic knob, where calcium quickly rises in response to odorants. All 4 isoforms are also found in the soma, where calcium rises last after stimulation. Here, by comparing the kinetics of $Ca^{2+}$ clearance in control OSNs and in those treated with PMCA and other inhibitors, we demonstrate that PMCAs contribute to OSN poststimulation removal of $Ca^{2+}$. We also compare poststimulation rates of $Ca^{2+}$ removal in OSNs from wild-type and PMCA knockout mice (PMCA2 KO). We chose to work with the PMCA2 KO because sensory neurons are known to be affected in PMCA2 null mice, and the KO homozygote is viable (Shull et al. 2003; Prasad et al. 2004). Other PMCA KOs are embryonic lethal (PMCA1), display sperm motility defects (PMCA4), or are not available (PMCA3). We demonstrate that, in addition to the $Na^+$/$Ca^{2+}$ exchanger (NCX) and ER $Ca^{2+}$ pump (SERCA), PMCAs contribute significantly to the removal of calcium from the knob after OSN stimulation. Studies of PMCA2 KO show that the loss of a single PMCA isoform results in a slower rate of $Ca^{2+}$ clearance and present a means by which we can test whether this loss affects the sense of smell.

## Materials and methods

### Animals

Guidelines set by the University's Laboratory Animal Care and Use Committee as well as by the National Institutes of Health Guide for the Care and Use of Laboratory Animals were followed for breeding and using animals for these experiments. Heterozygous C-57 Black Swiss mice ($Pmca2^{+/-}$) (gift from Dr Gary Shull, University of Cincinnati) carrying 1 null allele for PMCA2 and 1 allele normal for the PMCA2 isoform (Kozel et al. 1998) were bred in the University Animal Care Facility. The litters were genotyped at 3 weeks of age; wild-type ($Pmca2^{+/+}$) and PMCA2 KO ($Pmca2^{-/-}$) were marked with ear punches. We will use the term PMCA2 KO throughout.

### Solutions

Unless otherwise stated, all chemicals were purchased from Sigma-Aldrich (St Louis, MO). Mammalian Ringer's solution consisted of the following (in mM): 145 NaCl, 5 KCl, 1 $CaCl_2$, 1 $MgCl_2$, 1 pyruvic acid, 5 D-glucose, and 20 *N*-[2-hydroxyethyl]-piperazine-*N*′-[2-ethanesulfonic acid] (HEPES). For low-$Na^+$ Ringer's solution, NaCl was substituted with 145 mM choline chloride, and the pH was adjusted to 7.2 using approximately 8 mM NaOH. Dissociation solution contained the following (in mM): 145 NaCl, 5 KCl, 1 pyruvic acid, 1 ethylenediaminetetraacetic acid, 20 Na-free HEPES at pH 7.2, with 0.025 mg/ml papain, and 2 mM L-cysteine. Stop solution contained the following (in mM): 145 NaCl, 5 KCl, 2 $CaCl_2$, 1 $MgCl_2$, 20 Na-free HEPES, 5 glucose, 1 pyruvic acid, 0.1 mg/ml leupeptin (RPI, Mt Prospect, IL), and 0.01% bovine serum albumin at pH 7.2.

Isobutyl methylxanthine (IBMX) and 7-deacetyl-7-[-*O*-(*N*-methyl piperazino)-γ-butryl]-dihydrochloride (cell permeant forskolin) were obtained from Calbiochem (San Diego, CA) and used at 1 mM and 30 μM, respectively. Carboxyeosin (CE) and cyclopiazonic acid (CPA) stocks were made in dimethyl sulfoxide (DMSO) (4 and 10 mM, respectively), and the final concentrations were 10 and 5 μM for CE and CPA. The DMSO concentrations of these final solutions were 0.75% and 0.05% v/v, respectively. For PMCA inhibition, cells were treated with CE for 10 min along with fura-2 loading before being used for imaging. (Cells loaded with CE only were examined for fluorescence that would interfere with fura-2 fluorescence. We found no fluorescence from the CE-loaded cells.) Our working concentration of CE is within the range of concentrations of eosin that specifically inhibit all PMCA activity without affecting the NCX (Gatto et al. 1995). CE is regularly used for inhibition of PMCAs (e.g., Kurnellas et al. 2004), and we used a level well below that used by others on rat OSNs (Castillo et al. 2007). Eosin up to 20 μM does not inhibit the NCX (Gatto et al. 1995), and we used 10 μM CE. The $IC_{50}$ for eosin is 2-fold higher than for CE (Gatto and Milanick 1993). For the SERCA inhibition experiments, cells were continuously perfused with CPA during the experiment (Seidler et al. 1989). The bath solution was changed from normal Ringer's solution (145 mM $Na^+$) to low (8 mM) $Na^+$ for the NCX-reversal experiments.

### Dissociation of olfactory neurons

Adult Black Swiss C-57 mice were anesthetized and sacrificed by $CO_2$ asphyxiation and cervical dislocation. Olfactory epithelium along with the turbinates were dissected out and placed in 3 ml of "dissociation solution" with papain, after which they were gently cut into small pieces. To dissociate OSNs from supporting cells, the solution with the epithelia was gently triturated in a 5-ml glass tube with a fire-polished wide-bore glass pipette. The solution was kept at room temperature for 10 min followed by triturating 2 more times with smaller bore pipettes. It was then filtered through nylon mesh to remove any nondissociated tissue/bones. Papain activity in the cell suspension was halted using 3 ml of "stop solution" containing leupeptin.

### Fura-2 loading and calcium imaging

Dissociated cells were plated on a concanavalin A-coated (1 mg/ml) glass coverslip attached to a Warner perfusion chamber and allowed to settle for 10 min. An equal volume of a solution of 10 μM fura-2AM in Ringer's (diluted from a 1 mM stock in pure DMSO; Invitrogen, Eugene, OR) with 0.1% of the dispersing agent Pluronic F-127 (Invitrogen) was added to the cells in the dissociation and stop solutions (final concentration 5 μM fura-2AM, 0.05% Pluronic F-127, and 0.025% DMSO). (When the cells were loaded with CE, both fura-2AM with Pluronic F-127 and CE were added to the

cells together with a final DMSO concentration of 0.75%. For control conditions, the solutions were made and applied in the same way, but a DMSO solution without CE was substituted for the CE solution. Final concentration of CE was 10 μM. See above for stock solutions.) The cells were incubated for 20 min at room temperature before being imaged on a Nikon eclipse TE2000U inverted microscope fitted with a ×40 super fluor phase contrast objective. Cells were continuously perfused with mammalian Ringer's solution using a Warner perfusion system (Warner Instruments, Hamden, CT). Cells were exposed to alternating 340 and 380 nm light from a Xenon short-arc lamp through narrow band-pass filters, and the emission at 510 nm was recorded using a Hamamatsu ORCA-285 cooled CCD camera connected to a computer. Exposure time was 100 or 200 ms for both excitation wavelengths, and frame acquisitions were made every 3–8 s. Only cells with visible cilia were used for stimulation. The dendritic knob, dendrite, and soma of OSNs were monitored for changes in calcium levels by applying IBMX and forskolin stimulation for 8 s. Ratio values and pseudocolor images of the cells were recorded and analyzed using SimplePCI Ver.6 software (Hamamatsu Corporation, Sewickley, PA). To convert ratio values into $[Ca^{2+}]_i$, in vitro calibration was performed using the Molecular Probes Fura-2 Calcium Imaging Calibration Kit (F-6774). Intracellular $[Ca^{2+}]_i$ was calculated using the equation of Grynkiewicz et al. (1985):

$$\left[Ca^{2+}\right]_i = Kd\left[\left(R - Rmin\right)/\left[Rmax - R\right)\right]\beta$$

The parameter values were $R$ = F340/F380, $R$min = 0.55, $R$max = 19.96, β = 8.82, and fura-2 Kd = 309 nM.

In vivo measurements of $Ca^{2+}$ levels require the permeabilization of the cells and subsequent measurement of $R$min and $R$max values. We found the $R$max for the in vivo method difficult to achieve reliably and the in vitro method adequate to give us $Ca^{2+}$ values in line with published values (see Results). To avoid problems with $Ca^{2+}$ loading of the cell from repeated depolarizing stimulations, we analyzed the first $Ca^{2+}$ peak from the first stimulation only. All measurements were made at room temperature.

In all experiments, individual OSNs that had visible cilia were perfused with IBMX/forskolin for 8 s after which the bath flow cleared the perfusing solution. In each trial, we examined between 4 and 8 cells; the figure legends indicate the numbers of OSNs used for a particular experiment. We used IBMX with forskolin because we have found that together the 2 compounds increase the likelihood of eliciting a calcium transient in an OSN that is comparable to odor stimulation, and this combination is used commonly by other laboratories in OSN studies (e.g., Leinders-Zufall et al. 1997; Gomez et al. 2005; Zhang and Delay 2006; for review, see Kleene 2008). Durations of calcium transients from odor or IBMX/forskolin stimulation can be quite variable. However, the transients that we measured were within the published time frames of OSNs stimulated by IBMX/forskolin (Leinders-Zufall et al. 1997; Otsuguro et al. 2005; Gautam et al. 2006) or odor (Bozza and Kauer 1998; Gomez et al. 2005). We discuss peak heights in Results.

For all data sets, we used cells from at least 3 different mice. Differences among rate constants or average $Ca^{2+}$ levels were tested for significance using Student's $t$-test.

### Data analysis

The background-corrected ratio responses were normalized and curve fitted to a single exponential. Rate constants ($K$ values) were calculated for each trace utilizing 1-phase exponential decay analysis by Prism5 (GraphPad software Inc., San Diego, CA). Goodness of fit was monitored by the $R$ values for the curve, and data were not used if $R$ values were <0.95 (Prism5). $K$ values thus obtained were compared between wild-type and PMCA2 knockout OSNs as well as between control and treatment groups. Differences between experimental groups were analyzed using Student's $t$-test. A $P$ value of less than 0.05 was considered significant.

Single exponentials provided excellent fits ($R$ values >0.95). Although all curves could be assigned 2 exponentials, these $K$ values were much more variable among OSNs from a single animal and between experiments. Therefore, we have done what generally appears in the literature and analyzed single exponential decays (Pottorf and Thayer 2002; Ficarella et al. 2007). Only in CE-treated and PMCA2 KO OSN "cell bodies" stimulated with IBMX/forskolin did calcium not return back to baseline even after 12 min, instead usually attaining a new plateau. In these cases, even though we could calculate a $K$ value by fitting a single exponential, we did not because it would imply that OSNs in these situations clear calcium from cell bodies back to baseline. Therefore, the single exponential fit would not accurately model the effect of CE or the loss of PMCA2 on cell bodies.

### Immunofluorescence

Preparation of cells for deconvolution fluorescence microscopy and all materials and conditions were as described in Weeraratne et al. (2006). Preincubation with the pan-PMCA cognate peptide and omission of primary antibody were used as controls with no resulting immunofluorescence (results not shown).

## Results

### Calcium clearance from wild-type OSNs in the presence of PMCA inhibitor

When wild-type OSNs are stimulated with IBMX and forskolin to mimic the application of odor to the cilia, there is a rise in $Ca^{2+}$ in the knob, followed temporally by a rise in the dendrite and finally a rise in the cell body (Figure 1A). The PMCA inhibitor eosin can specifically inhibit PMCAs

without affecting the NCX (Gatto et al. 1995). We used CE that has a 2-fold lower $IC_{50}$ than eosin (Gatto and Milanick 1993) at a concentration well within the eosin concentration range that leaves the NCX unaffected. When IBMX/forskolin was used as the stimulus for the transduction pathway, the cell bodies of wild-type OSNs treated with CE did not return $Ca^{2+}$ to baseline within 12 min but rather plateaued at a new and higher baseline, whereas the DMSO-treated cell bodies consistently returned $Ca^{2+}$ to baseline (Figure 1B). In contrast, the knobs of both control- and CE-treated wild-type OSNs returned $Ca^{2+}$ to baseline, but the rate was significantly slower for the CE-treated OSN knobs than for control knobs (Figure 1C).

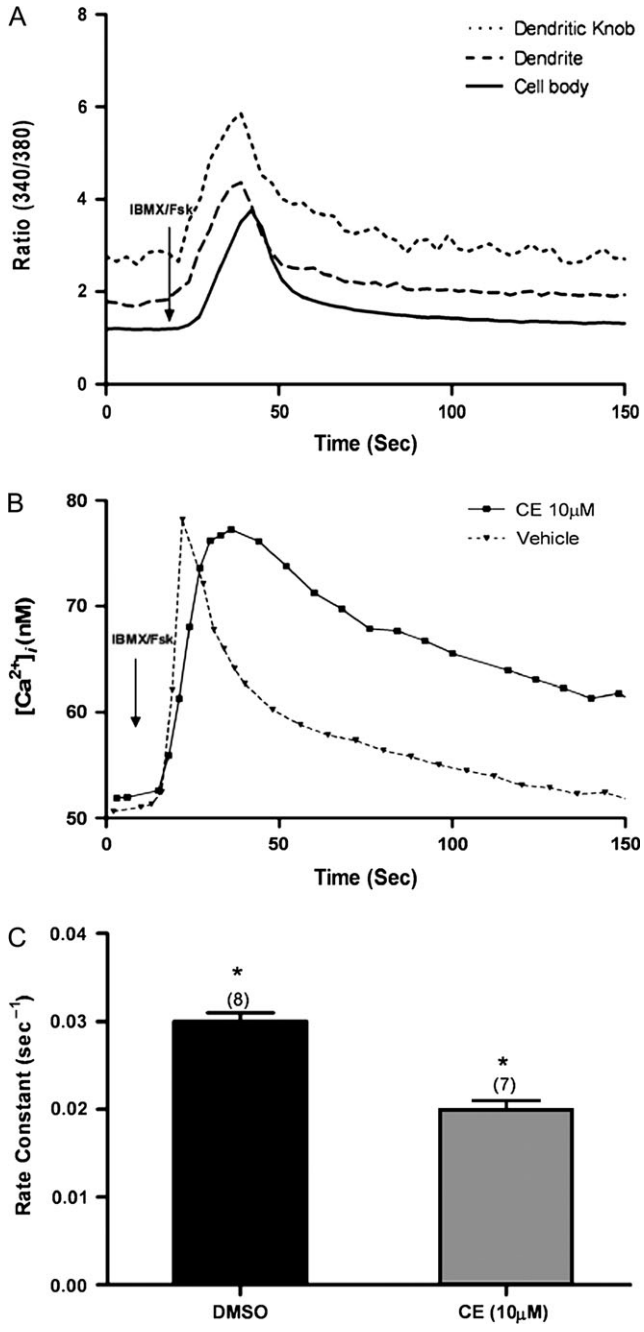


**Figure 1** Rate constants and $Ca^{2+}$ levels in OSNs treated with CE and stimulated with IBMX/forskolin. **(A)** Typical traces from an OSN showing the sequential elevation of calcium from the dendritic knob to the cell body when stimulated with IBMX/forskolin for 8 s. **(B)** $Ca^{2+}$ levels following 8 s of IBMX/forskolin treatment in control and CE-treated wild-type (WT) cell body. **(C)** Rate constants for $Ca^{2+}$ clearance following 8 s of IBMX/forskolin stimulation in the dendritic knobs of CE-treated OSNs are significantly smaller than in control-treated knobs (*) (DMSO $n = 8$ OSNs; CE $n = 7$ OSNs) ($P < 0.05$). Error bars represent the SEM.

### Compromising NCX and SERCA

Treatment of wild-type OSNs with CPA to inhibit the SERCA caused a significant decrease in the rate of $Ca^{2+}$ clearance from wild-type OSNs. Both cell bodies (Figure 2A) and knobs (Figure 2B) of CPA-treated OSNs showed slower clearance than control OSNs following stimulation with IBMX/forskolin.

Previously, the NCX was demonstrated to be present in mouse, rat, and frog OSNs and to play a role in $Ca^{2+}$ clearance in OSNs (Jung et al. 1994; Reisert and Matthews 1998; Castillo et al. 2007; Pyrski et al. 2007). To keep the NCX from removing $Ca^{2+}$ from the OSN, we recorded wild-type OSNs in low-$Na^{+}$ (8 mM) Ringer's solution. $Ca^{2+}$ would

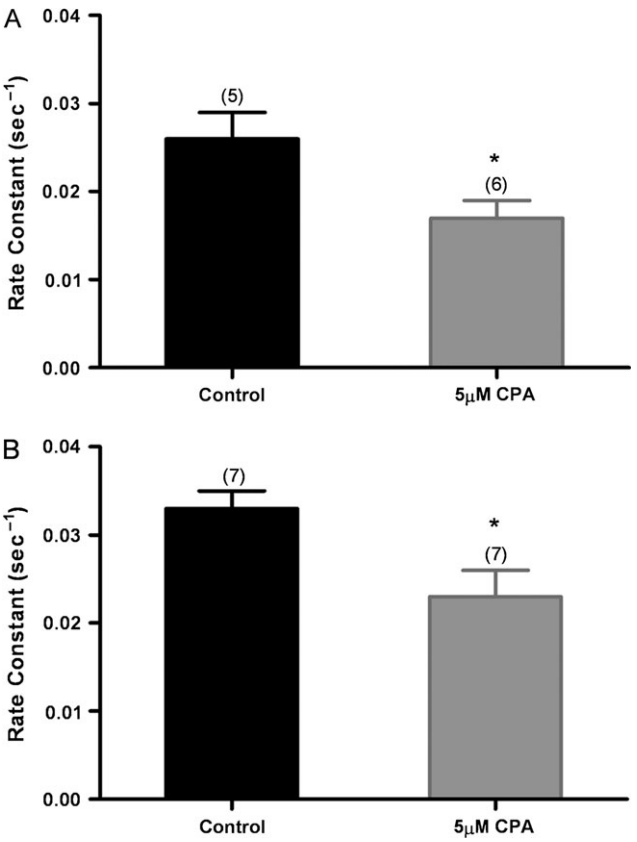


**Figure 2** Effect of SERCA inhibition on calcium clearance. In response to 8 s of IBMX/forskolin stimulation, the CPA-treated OSNs show slower $Ca^{2+}$ clearance from cell bodies **(A)** and knobs **(B)** compared with control-treated OSNs (*$P < 0.05$). Error bars represent the SEM. Numbers are averages of 5–7 OSNs ± SEM.

typically rise in OSNs in this solution (Jung et al. 1994), and when the baseline stabilized, we stimulated the cells with IBMX/forskolin. We observed that the rate of clearance was significantly reduced in both cell bodies and knobs (Figure 3A,B). Note that the control rate constant for the cells in Figure 3B was significantly higher than the control rate constants in Figures 1 and 2. The low-$Na^+$ experiments did not require the addition of DMSO beyond that used for loading the fura-2 dye, whereas the experiments with CE and CPA required exposure of the control and test cells to additional DMSO in solution (see Materials and methods). Therefore, we carried out the low-$Na^+$ experiments again, with OSNs exposed to an additional 0.75% DMSO solution as though they were being loaded with CE. The *K* values for these knobs of OSNs treated with additional DMSO were 0.030 ± 0.002 and 0.021 ± 0.001 standard error of the mean (SEM) in normal Ringer's and in low-$Na^+$ Ringer's, respectively. (Note in Table 1 that the *K* values for the normal Ringer's control for the low-Ringer's experiment and the control for the CE experiment are the same, as we would expect.)

### Combination of conditions

We show in Table 1 that the rate of clearance of $Ca^{2+}$ from the dendritic knob is about equally affected by the 3 different conditions that we applied to wild-type OSNs. (The cell bodies were affected as well, but because CE-treated cell bodies did not return to baseline, we could not dependably calculate the rate of a clearance that would restore original $Ca^{2+}$ levels.) To determine whether the inhibitors and low-$Na^+$ conditions were effectively eliminating and not just reducing the contribution of pumps or the exchanger, we carried out combination experiments in which both inhibitors and low-$Na^+$ conditions were combined in series (Figure 4). The cells were loaded with CE and treated with CPA before being exposed

**Table 1** Changes in rate constants for $Ca^{2+}$ clearance from the dendritic knob following IBMX/forskolin stimulation from wild-type OSNs treated with CE, CPA, or low-$Na^+$ Ringer's

| Condition | *K* value per seconds (control) | *K* value per seconds (test) | Percent reduction (%) |
|---|---|---|---|
| CE (PMCA) | 0.030 ± 0.001 | 0.020 ± 0.001 | 34 |
| CPA (SERCA) | 0.033 ± 0.002 | 0.023 ± 0.003 | 30 |
| Low $Na^+$ (NCX) | 0.030 ± 0.002 | 0.021 ± 0.001 | 30 |

Control and test OSNs for the low-$Na^+$ experiment were treated with an additional DMSO during the loading of fura-2AM to mimic the control for the CE experiment (see Materials and methods). Data are averages of 5–8 cells ± SEM.

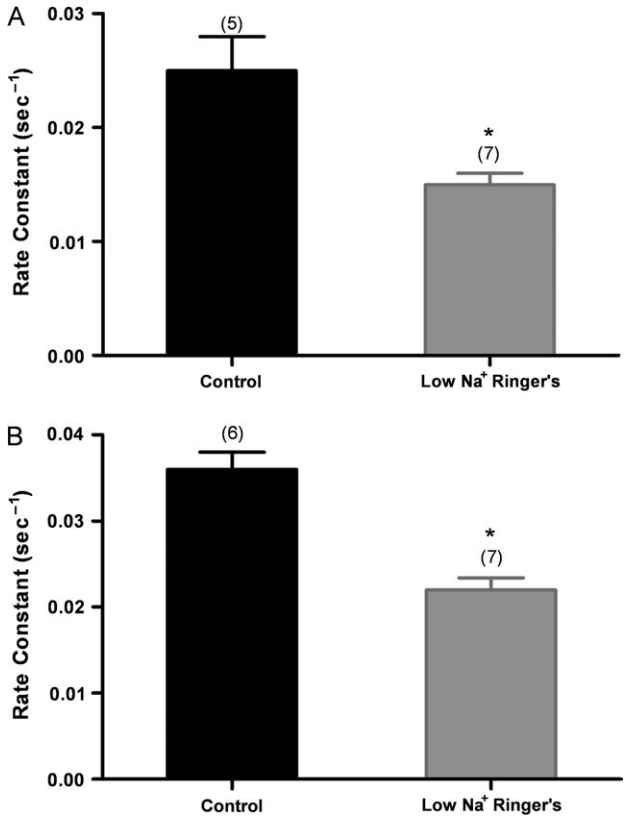


**Figure 3** Effect of low-$Na^+$ conditions to reverse NCX activity on $Ca^{2+}$ clearance after IBMX/forskolin stimulation. **(A)** Wild-type OSNs treated for 8 s with IBMX/forskolin in low-$Na^+$ Ringer's show a significantly slower calcium clearance from the cell body compared with control OSNs in normal Ringer's; **(B)** similarly treated OSNs show a significantly slower calcium clearance from the knobs compared with control OSNs in normal Ringer's (*$P < 0.05$). Error bars represent the SEM. Numbers are averages of 5–7 OSNs ± SEM.

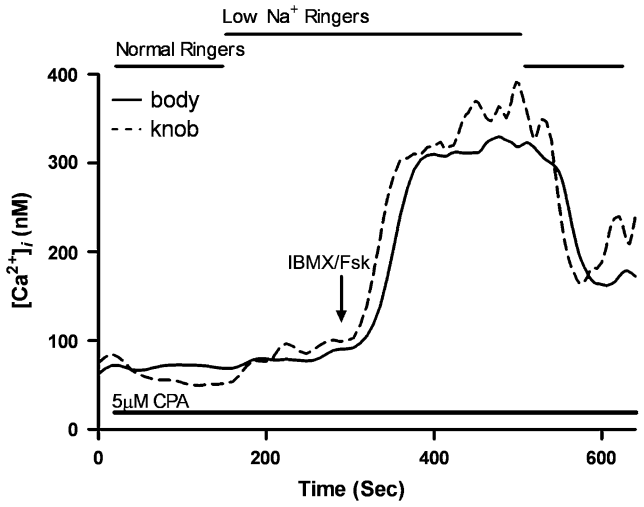


**Figure 4** Calcium levels of an OSN treated with 2 inhibitors and low-$Na^+$ conditions and stimulated with IBMX/forskolin for 8 s. Cells were loaded with 10 μM CE for 10 min along with fura-2. The cells were continuously perfused with 5 μM CPA throughout the experiment. Bath solution was switched to 8 mM $Na^+$ Ringer's with CPA, and IBMX/Fsk stimulation was applied for 8 s after a new baseline stabilized. The bath solution was switched back to normal Ringer's with CPA after 200 s. The recording shown is a representative result from 4 cells.

to low-$Na^+$ Ringer's solution. Once the rise in baseline $Ca^{2+}$ stabilized from the reversal of the exchanger, we applied IBMX/forskolin. The rise in $Ca^{2+}$ in both the knob and cell body did not decline unless we replaced normal Ringer's solution. Even then, neither the cell knob nor body cleared the $Ca^{2+}$ back to the original baseline. Instead, $Ca^{2+}$ remained high for as long as we could record. Figure 4 shows a typical set of results from these experiments.

### PMCA2 knockout OSNs show no PMCA2 in immunofluorescence studies

We previously demonstrated the presence of PMCA isoforms 1–4 in wild-type OSNs using pan-specific and isoform-specific antibodies (Weeraratne et al. 2006). PMCA1 was found to be distributed along the length of the entire cell from cilia to dendritic knob to dendrite to cell body. PMCA2 was similarly distributed but with less staining in the dendrite than shown by cells labeled with the other 3 isoform-specific antisera. PMCA3 antibody showed no recognition of epitopes in the cilia, but otherwise stained the entire cell. PMCA4 was found in cilia, knob, and cell body but very little was found in the dendrite.

Here we show a PMCA2 KO cell treated with the pan-antibody against all 4 isoforms and anti-adenylyl cyclase III, a marker for cilia (Figure 5B,C,D). A differential interference contrast optics (DIC) image of the cell is shown in Figure 5A. As a control for the pan-PMCA antibody, the antibody was preabsorbed with the cognate peptide, and we saw no immunofluorescence from these cells (data not shown). We previously published in Weeraratne et al. (2006) a similar image of the wild-type OSN with the pan-PMCA antibody and also images of wild-type OSNs with 4 different isoform-specific antibodies to demonstrate that all 4 are expressed. In contrast, Figure 5 shows a typical result for a PMCA2 KO OSN (Figure 5E, DIC image) treated with the anti-PMCA2 antibody (Figure 5F). No fluorescence is visible. The PMCA2 KO cells show antibody labeling of wild-type OSNs with anti-PMCA1, 3, and 4 antibodies, but for brevity, we show here only the results with antibodies to PMCA2 and pan-PMCA.

### PMCA2 KO OSNs show slower calcium clearance

The rate of clearance is clearly faster from the wild-type OSN cell bodies than from PMCA2 KO cell bodies (Figure 6A). The PMCA2 KO OSN cell bodies fail to return their $Ca^{2+}$ levels to baseline after IBMX/forskolin stimulation. However, wild-type and PMCA2 KO OSNs clear $Ca^{2+}$ from "knobs" back to the level of baseline after IBMX/forskolin stimulation, and the $K$ values show that the wild-type OSNs clear $Ca^{2+}$ significantly faster from knobs than PMCA2 KO OSNs (Figure 6B).

### Basal calcium levels are similar in wild-type and PMCA2 KO OSNs

The basal $Ca^{2+}$ levels in wild-type and PMCA2 KO OSNs were estimated from fura-2 ratios compared with an in vitro calibration curve. By this method, we found that wild-type and PMCA2 KO OSNs had very similar levels of $Ca^{2+}$ (Figure 7). Although the PMCA2 KO levels were slightly higher, they were not significantly so. The range of $Ca^{2+}$ in the cells was very large but consistent with both the average $Ca^{2+}$ levels and ranges found in previous measurements (Restrepo et al. 1993).

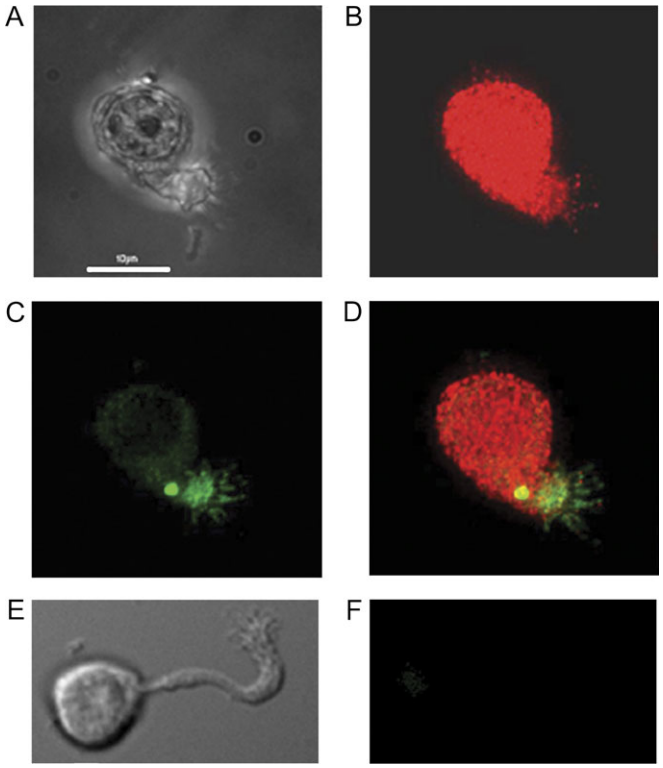


**Figure 5** Immunofluorescence of isolated PMCA2 KO olfactory neurons. **(A)** DIC image, **(B)** labeled with pan-PMCA, **(C)** labeled with anti-adenylyl cyclase III, **(D)** and merged image. **(E)** DIC image of another PMCA2 KO OSN. **(F)** Immunofluorescence of same cell labeled with anti-PMCA2 antibody demonstrates that it lacks PMCA2. Scale bar = 10 μm. These images are representative of the OSNs we examined.

### Peak heights

Interestingly, the peak heights of the calcium transients in wild-type OSNs stimulated with IBMX/forskolin (peak 218 ± 39 nM; amplitude [net change] 166 ± 40 nM SEM, $n$ = 23) were very similar to those of the KO OSNs (peak 214 ± 10 nM; amplitude 161 ± 10 SEM, $n$ = 7). Because there is no significant difference in peak heights or amplitudes between wild-type and PMCA2 KO OSNs, PMCA2 appears to shape the $Ca^{2+}$ signal by affecting its duration.

Although these IBMX/forskolin-stimulated changes in $Ca^{2+}$ in the knob may seem small, they are consistent with those in salamander cilia caused by IBMX (80 nM net change above a basal level of 40–80 nM) or odorants (20–300 nM net change above a basal level of 40 nM) (Leinders-Zufall et al. 1997, 1998). All these peak responses to IBMX/forskolin are below the micromolar levels needed

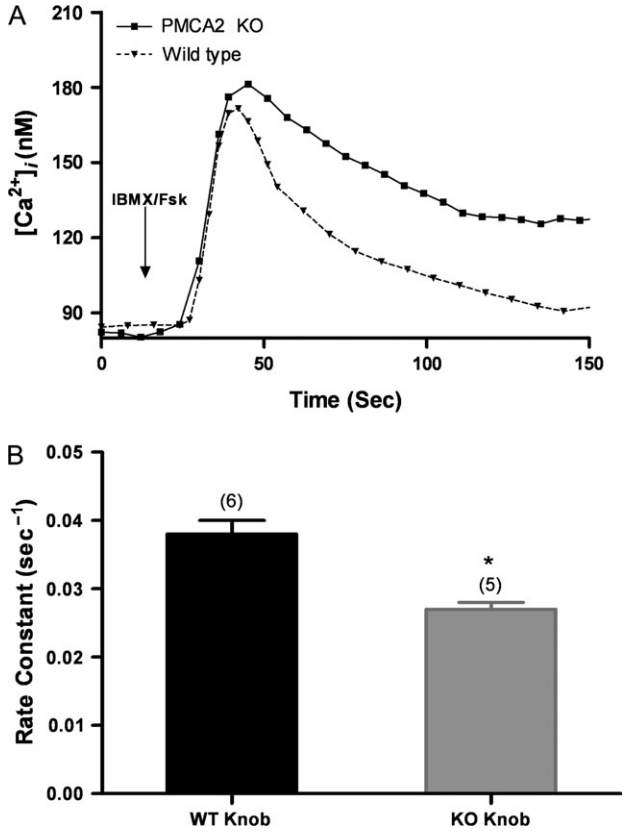


**Figure 6** Rate constants and $Ca^{2+}$ levels from wild-type (WT) and PMCA2 KO cells stimulated with IBMX/forskolin for 8 s. **(A)** Calcium levels from WT and PMCA2 KO cell bodies stimulated with IBMX/forskolin. **(B)** Rate constants for WT and PMCA2 KO dendritic knobs after IBMX/forskolin stimulation show a significant difference (WT $n = 6$ OSNs; KO $n = 5$ OSNs) (*$P < 0.05$). Error bars represent the SEM.

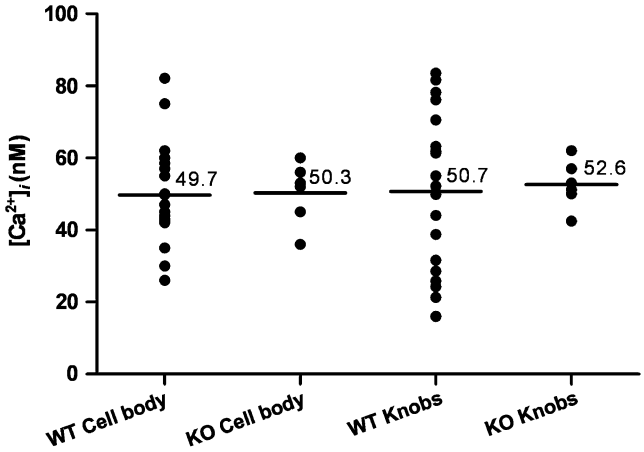


**Figure 7** Basal calcium levels in wild-type (WT) and PMCA2 KO OSNs. Measurements from individual cell are shown as well as the "average" (line) for each cell type's cell body or knob (WT: cell body $n = 20$, knob $n = 24$; KO: cell body $n = 66$, knob $n = 6$). There are no significant differences between WT and PMCA2 KO OSNs.

to open the $Cl^-$ channels to amplify the odor-evoked current (Reisert et al. 2003). However, others have made similar observations and speculated that there are microdomains in cilia where $Ca^{2+}$ rises to levels sufficient to mediate odor adaptation through the CNGC (Leinders-Zufall et al. 1998) and possibly activate the $Cl^-$ channels (Reisert et al. 2003).

## Discussion

We present a kinetic analysis to elucidate a role for PMCAs in $Ca^{2+}$ clearance from OSNs by monitoring the decay of the $Ca^{2+}$ signal in cell bodies and knobs following stimulation with IBMX/forskolin to open CNGCs and initiate the odor pathway downstream of the receptors. The $Ca^{2+}$ transient from odor transduction begins in the cilia and rapidly involves the knob, but because we are not able to image the short cilia of mammalian OSNs, we focus on knobs for measuring the rates of $Ca^{2+}$ removal. Because CNGCs are found in the knob and are not limited to the cilia (Firestein et al. 1991; Kurahashi and Kaneko 1991), we feel that the knob is a useful proxy for the cilia. Receptors and $Cl^-$ channels, likewise, are not limited to the cilia (Hallani et al. 1998; Strotmann et al. 2004). Knobs have provided important odor-specific information on $Ca^{2+}$ transients in whole epithelium as well as in isolated OSNs (Firestein et al. 1991; Leinders-Zufall et al. 1997; Ma and Shepherd 2000).

Our data are consistent with those previously published. OSNs stimulated with IBMX/forskolin solution show a temporal pattern of $Ca^{2+}$ rise in the knob, followed sequentially by increases in the dendrite and cell body (Figure 1A), reminiscent of the pattern found by Leinders-Zufall et al. (1997) for salamander OSNs after IBMX stimulation. Others have found that $Ca^{2+}$ clearance slows with NCX reversal in low-$Na^+$ conditions (Jung et al. 1994; Reisert and Matthews 1998; Castillo et al. 2007). Given that baseline free $Ca^{2+}$ levels in rat, mouse, and frog OSNs are <100 nM (Restrepo et al. 1993; Jung et al. 1994; Leinders-Zufall et al. 1997; and this report [Figures 1A and 6A]), we expect that the NCX will clear $Ca^{2+}$ down to 1–0.1 μM, and the PMCAs will clear $Ca^{2+}$ to the OSN basal level because PMCAs have a higher affinity for $Ca^{2+}$ than the NCX (Carafoli 1994).

From rate constants (Figure 6A,B), we see that the PMCA2 KO OSN does not clear $Ca^{2+}$ as quickly as wild-type cells from the knob or cell body following IBMX/forskolin stimulation. The most dramatic contrast between wild-type and PMCA2 KO OSNs is in the failure of the PMCA2 KO OSN cell bodies to return $Ca^{2+}$ to baseline after IBMX/forskolin stimulation (Figure 6A). Therefore, the absence of this single PMCA isoform can lead to measurable changes in $Ca^{2+}$ clearance with a treatment that simulates odor stimulation and transduction. Even though the PMCA2 KO OSNs have 3 other PMCAs in the knob, 2 in the dendrite and 3 in the cell body, there remain measurable differences in clearance rates. This lack of PMCA redundancy has been observed in other neuronal systems (Shull et al. 2003). The clearance rates for the PMCA2 KO OSNs were slightly but

significantly faster than rates for wild-type OSNs treated with CE, which should inhibit all 4 PMCAs. We have no evidence that the level of CE we use inhibits all the PMCAs, but because we can account for almost all the calcium clearance with a combination of CE, CPA, and low-$Na^+$ bath conditions, it is likely that we have inhibited all the PMCAs. We conclude that PMCA2 is a major contributor to calcium clearance from the knob.

The differences between PMCA2 KO and wild-type OSN clearance are probably not due to differences in the basal levels of $Ca^{2+}$, which are very similar (Figure 7). The average values that we measure are quite close to those reported by Restrepo (83 ± 57 nM in the soma; 77 ± 71 nM in the knob) for rat OSNs. The basal levels show large ranges for both wild-type and PMCA2 KO, but these ranges are consistent with those found by Restrepo et al. (1993) for rat.

The PMCA inhibitor CE significantly slowed the rate of $Ca^{2+}$ clearance from wild-type OSN cell bodies and knobs following IBMX/forskolin stimulation (Figure 1). CE-treated wild-type OSNs (Figure 1B) fail to return $Ca^{2+}$ to basal levels, whereas the knobs of the same cells remove $Ca^{2+}$ to basal levels, albeit more slowly than controls. The differences between cell bodies and knobs may be due to the proximity of the PMCAs to the source of $Ca^{2+}$ influx.

SERCA inhibitor CPA and low-$Na^+$ Ringer's slowed the rates of $Ca^{2+}$ clearance from the wild-type OSN cell bodies and knobs after IBMX/forskolin stimulation (Figures 2 and 3). Therefore, from our studies, it appears that there are at least 3 $Ca^{2+}$ clearance mechanisms at work in the OSN: PMCAs, SERCA, and the NCX. Compromising each mechanism separately reduces the rate of clearance from the knob after IBMX/forskolin stimulation by about 30–34% (Table 1). We cannot attribute a precise share to each mechanism for the total clearance of $Ca^{2+}$ from the knob because we have no direct evidence that our inhibition of PMCAs or SERCA or reversal of NCX is complete. However, when we combined the inhibitors of PMCA and SERCA and used low-$Na^+$ conditions to prevent NCX from removing $Ca^{2+}$, we found that OSNs' ability to remove $Ca^{2+}$ from the knob after simulation was greatly reduced (Figure 4).

A neuron's repertoire of PMCA isoforms and splice variants shapes its $Ca^{2+}$ signal amplitude and speed of return to baseline and thus shapes the neuron's response (Brini et al. 2007). "Fast pumps" contribute to a "fast cell," that is, a cell with a fast decaying $Ca^{2+}$ signal (Caride, Filoteo, et al. 2001). Rates of activation of the PMCAs are determined by the rate of reaction with $Ca^{2+}$–calmodulin and the level of basal activity in the absence of calmodulin. Other considerations in shaping a $Ca^{2+}$ transient are the magnitude of activation relative to basal activity and the PMCA inactivation rate (Caride et al. 2007). We know from reverse transcriptase–polymerase chain reaction that all 4 isoforms are present in mouse OSNs, and the splice variants are PMCA1b, PMCA2b, PMCA3b, and PMCA4a (Weeraratne et al. 2006), with PMCA1, 2b, and 4a in the cilia and all 4 of the PMCAs in the knob. (An "a" or "b" indicates the splice variant in the calmodulin-binding domain, which determines much of the activation rate.) PMCA1 is considered housekeeping and constitutive (Okunade et al. 2004), but PMCA2b and 4a are dynamic and could shape the $Ca^{2+}$ transient resulting from odor stimulation in the cilia and knob. PMCA3b is neuron specific and activated by $Ca^{2+}$/calmodulin, but less is known about its kinetics (Caride, Filoteo, et al., 2001; Strehler and Zacharias 2001; Strehler et al. 2007).

Given the PMCAs in the mouse OSN, the cilia and knob should show an "intermediate" phenotype for ending a $Ca^{2+}$ transient because PMCA2b and 4a are intermediate in their rate of activation. Both show modest activation by calmodulin and almost identical rate constants, but overall PMCA4a is slightly faster to activate than 2b (Caride, Filoteo, et al. 2001). The inactivation rate for PMCA4a is also intermediate and faster than the slowest, PMCA4b (Caride et al. 1999). Based on our measurements, we see that the OSN knob and cell body $\tau$ values for clearance are around 30 s (from Table 1, $\tau = 1/K$), consistent with the half-time for decay of the $Ca^{2+}$ transient from intermediate Jurkat cells (22–107 s) (Caride, Filoteo, et al. 2001). (PMCA3b is thought to be intermediate as well and slower than isoform 3f. However, less is known about its kinetics [Caride, Filoteo et al. 2001; Strehler et al. 2007].)

PMCA2b is described as having a "memory" for past $Ca^{2+}$ transients because it quickly activates upon subsequent $Ca^{2+}$ transients (Caride, Filoteo, et al. 2001; Caride, Penheiter, et al. 2001). We predict that the loss of PMCA2 in KO OSNs would not only slow the clearance of the $Ca^{2+}$ transient but also that the KO cells respond less quickly than normal to a second round of odor stimulation because the missing PMCA2b has a longer memory than 4a. We expect that loss of PMCA2 would not affect the amplitude of the transient because the remaining PMCA4a is faster to activate than PMCA2b and might be more responsible for shaping the early part of the transient; we have found that the amplitudes of $Ca^{2+}$ transients in wild-type and KO show no significant difference. The loss of specific PMCAs should also be reflected in adaptation kinetics because it has been demonstrated that the most important contributor to fast adaptation in the OSN is the feedback of $Ca^{2+}$/calmodulin onto the CNGC (Kurahashi and Menini 1997; Boccaccio et al. 2006; for review, see Zimmerman 2006).

Previously we (Weeraratne et al. 2006) and more recently Castillo et al. (2007) demonstrated that PMCAs are expressed both in mouse and rat OSNs. Castillo and coworkers used the pan-antibody to demonstrate that PMCAs in general are expressed in rat OSN cilia, which concurs with our results using pan- and isoform-specific antibodies in mouse OSNs. Castillo and coworkers used vesicles and electrophysiology to demonstrate a CE-sensitive ATP-dependent ciliary $Ca^{2+}$ transport that is attributable to the PMCAs. They also modified the $Na^+$ environment to reverse the NCX and

demonstrated a role for the NCX in $Ca^{2+}$ clearance from the cilia. Whereas we have taken a different approach to studying $Ca^{2+}$ clearance from the knob and cell body, the Castillo group's results in rat support our analysis of mouse OSN kinetics.

In summary, we have identified PMCAs as contributing to a major clearance mechanism and also elucidated the relative contributions of PMCAs, SERCA, and NCX to $Ca^{2+}$ removal from OSNs. More importantly, we can now explore the contribution of PMCAs to the shape and duration of the $Ca^{2+}$ transient in mouse OSNs, including PMCA4 through studies of PMCA4 KO.

## Funding

National Institutes of Health DC 0066463; National Center for Research Resources P20 RR016435-06 for imaging.

## Acknowledgements

We thank Dr G. Shull for the PMCA2 KO and Drs Jerome Fiekers and George Wellman for advice.

## References

Bakalyar HA, Reed RR. 1990. Identification of a specialized adenylyl cyclase that may mediate odorant detection. Science. 250:1403–1406.

Boccaccio A, Lagostena L, Hagen V, Menini A. 2006. Fast adaptation in mouse olfactory sensory neurons does not require the activity of phosphodiesterase. J Gen Physiol. 128:171–184.

Borisy FF, Ronnett GV, Cunningham AM, Juilfs D, Beavo J, Snyder SH. 1992. Calcium/calmodulin-activated phosphodiesterase expressed in olfactory receptor neurons. J Neurosci. 12:915–923.

Bozza TC, Kauer JS. 1998. Odorant response properties of convergent olfactory receptor neurons. J Neurosci. 18:4560–4569.

Bradley J, Reuter D, Frings S. 2001. Facilitation of calmodulin-mediated odor adaptation by cAMP-gated channel subunits. Science. 294:2176–2178.

Brini E, DiLeva F, Domi T, Fedrizzi L, Lim D, Carafoli E. 2007. Plasma-membrane calcium pumps and hereditary deafness. Biochem Soc Trans. 35:913–918.

Carafoli E. 1994. Biogenesis: plasma membrane calcium ATPase: 15 years of work on the purified enzyme. FASEB J. 8:993–1002.

Caride AJ, Elwess NL, Verma AK, Filoteo AG, Enyedi A, Bajzer Z, Penniston JT. 1999. The rate of activation by calmodulin of isoform 4 of the plasma membrane $Ca^{2+}$ pump is slow and is changed by alternative splicing. J Biol Chem. 274:35227–35232.

Caride AJ, Filoteo AG, Penheiter AR, Paszty K Enyedi A, Penniston JT. 2001. Delayed activation of the plasma membrane calcium pump by a sudden increase in $Ca^{2+}$: fast pumps reside in fast cells. Cell Calcium. 30:49–57.

Caride AJ, Filoteo AG, Penniston JT, Strehler EE. 2007. The plasma membrane $Ca^{2+}$ isoform 4a differs from isoform 4b in the mechanism of calmodulin binding and activation kinetics. J Biol Chem. 282: 25640–25648.

Caride AJ, Penheiter AR, Filoteo AG, Bajzer Z, Enyedi A, Penniston JT. 2001. The plasma membrane calcium pump displays memory of past calcium spikes. J Biol Chem. 276:39797–39804.

Castillo K, Delgado R, Bacigalupo J. 2007. Plasma membrane $Ca^{2+}$-ATPase in the cilia of olfactory receptor neurons: possible role in $Ca^{2+}$ clearance. Eur J Neurosci. 16:2524–2531.

Choi EJ, Xia Z, Storm DR. 1992. Stimulation of the type III olfactory adenylyl cyclase by calcium and calmodulin. Biochemistry. 31:6492–6498.

Ficarella R, DiLeva F, Bortolozzi M, Ortolano S, Donaudy F, Petrillo M, Melchionda S, Lelli A, Domi T, Fedrizzi L, Lim D, et al. 2007. A functional study of plasma-membrane calcium-pump isoform 2 mutants causing digenic deafness. Proc Natl Acad Sci USA. 103:1516–1521.

Firestein S, Zufall F, Shepherd GM. 1991. Single odor-sensitive channels in olfactory receptor neurons are also gated by cyclic nucleotides. J Neurosci. 11:3565–3572.

Gatto C, Hale CC, Xu W, Milanick MA. 1995. Eosin, a potent inhibitor of the plasma membrane Ca pump, does not inhibit the cardiac Na-Ca exchanger. Biochemistry. 34:965–972.

Gatto C, Milanick MA. 1993. Inhibition of the red blood cell calcium pump by eosin and other fluorescein analogues. Am J Physiol. 264:C1577–C1586.

Gautam SH, Orsuguro K, Ito S, Saito T, Habara Y. 2006. Intensity of odorant stimulation affects mode of $Ca^{2+}$ dynamics in rat olfactory receptor neurons. Neurosci Res. 55:410–420.

Gautam SH, Otsuguro K-I, Ito S, Saito T, Habara Y. 2007. T-type $Ca^{2+}$ channels contribute to IBMX/forskolin- and $K^{+}$-induced transients in porcine olfactory receptor neurons. Neurosci Res. 57:129–139.

Gomez G, Lischka FW, Haskins ME, Rawson NE. 2005. Evidence for multiple calcium response mechanisms in mammalian olfactory receptor neurons. Chem Senses. 30:317–326.

Grynkiewicz G, Poenie M, Tsien RY. 1985. A new generation of Ca2+ indicators with greatly improved fluorescence properties. J Biol Chem. 260(3):440–3450.

Hallani M, Lynch JW, Barry PH. 1998. Characterization of calcium-activated chloride channels in patches excised from the dendritic knob of mammalian olfactory receptor neurons. J Membr Biol. 161:163–171.

Jung A, Lischka FW, Engel J, Schild D. 1994. Sodium/calcium exchanger in olfactory receptor neurons of *Xenopus laevis*. Neuroreport. 5:1741–1744.

Kleene SJ. 1993. Origin of the chloride current in olfactory transduction. Neuron. 11:123–132.

Kleene SJ. 2008. The electrochemical basis of odor transduction in vertebrate olfactory cilia. Chem Senses. 33:839–859.

Kozel PJ, Friedman RA, Erway LC, Yamoah EN, Liu LH, Riddle T, Duffy JJ, Doetschman T, Miller ML, Cardell EL, et al. 1998. Balance and hearing deficits in mice with a null mutation in the gene encoding plasma membrane Ca2+-ATPase isoform 2. J Biol Chem. 273:18693–18696.

Kurahashi T, Kaneko A. 1991. High density cAMP-gated channels at the ciliary membrane in the olfactory receptor cell. Neuroreport. 2:5–8.

Kurahashi T, Menini A. 1997. Mechanism of odorant adaptation in the olfactory receptor cell. Nature. 385:725–729.

Kurnellas MP, Nicot A, Shull GE, Elkabes S. 2004. Plasma membrane calcium ATPase deficiency causes neuronal pathology in the spinal cord: a potential mechanism for neurodegeneration in multiple sclerosis and spinal cord injury. FASEB J. express article doi: 10.1096/fj.04–2549fje.

Lagostena L, Menini A. 2003. Whole-cell recordings and photolysis of caged compounds in olfactory sensory neurons isolated from the mouse. Chem Senses. 28:705–716.

Leinders-Zufall T, Greer CA, Shepherd GM, Zufall F. 1998. Imaging odor-induced calcium transients in single olfactory cilia: specificity of activation and role in transduction. J Neurosci. 18:5630–5639.

Leinders-Zufall T, Ma M, Zufall F. 1999. Impaired odor adaptation in olfactory receptor neurons after inhibition of $Ca^{2+}$/calmodulin kinase II. J Neurosci. 19RC19: 1–6.

Leinders-Zufall T, Rand MN, Shepherd GM, Greer CA, Zufall F. 1997. Calcium entry through cyclic nucleotide-gated channels in individual cilia of olfactory receptor cells: spatiotemporal dynamics. J Neurosci. 17: 4136–4148.

Ma M, Shepherd GM. 2000. Functional mosaic organization of mouse olfactory receptor neurons. Proc Natl Acad Sci USA. 97:12869–12874.

Okunade GW, Miller ML, Pyne GJ, Sutlif RL, O'Connor KT, Neumann JC, Adringa A, Miller DA, Prasad V, Doetschman R, et al. 2004. Targeted ablation of plasma membrane $Ca^{2+}$-ATPase (PMCA) 1 and 4 indicates a major housekeeping function for PMCA1 and a critical role in hyperactivated sperm motility and male fertility for PMCA4. J Biol Chem. 279:33742–33750.

Otsuguro K-I, Guatam SH, Ito S, Habara Y, Saito T. 2005. Characterization of forskolin-induced $Ca^{2+}$ signals in rat olfactory receptor neurons. J Pharmacol Sci. 97:510–518.

Pottorf WJ, Thayer SA. 2002. Transient rise in intracellular calcium produces a long-lasting increase in plasma membrane calcium pump activity in rat sensory neurons. J Neurochem. 83:1002–1008.

Prasad V, Okunade GW, Miller M, Shull GE. 2004. Phenotypes of SERCA and PMCA knockout mice. Biochem Biophys Res Commun. 322: 1192–1203.

Pyrski M, Koo JH, Polumuri SK, Ruknudin AM, Margolis JW, Schulze DH, Margolis FL. 2007. Sodium/calcium exchanger expression in the mouse and rat olfactory systems. J Comp Neurol. 501:944–958.

Reisert J, Bauer PJ, Yau K-W, Frings S. 2003. The Ca-activated Cl channel and its control in rat olfactory receptor neurons. J Gen Physiol. 122: 349–363.

Reisert J, Matthews HR. 1998. $Na^{+}$-dependent $Ca^{2+}$ extrusion governs response recovery in frog olfactory receptor cells. J Gen Physiol. 112: 529–535.

Restrepo D, Okada Y, Teeter JH. 1993. Odorant-regulated $Ca^{2+}$ gradients in rat olfactory neurons. J Gen Physiol. 102:907–924.

Ronnett GV, Moon C. 2002. G proteins and olfactory signal transduction. Annu Rev Physiol. 64:189–222.

Schild D, Restrepo D. 1998. Transduction mechanisms in vertebrate olfactory receptor cells. Physiol Rev. 78:429–466.

Seidler NW, Jona I, Vegh M, Martonosi A. 1989. Cyclopiazonic acid is a specific inhibitor of the Ca2+-ATPase of sarcoplasmic reticulum. J Biol Chem. 264:17816–17823.

Shull GE, Okunade G, Liu LH, Kozel P, Periasamy M, Lorenz JN, Prasad V. 2003. Physiological functions of plasma membrane and intracellular Ca2+ pumps revealed by analysis of null mutants. Ann N Y Acad Sci. 986:453–460.

Strehler EE, Filoteo AG, Penniston JT, Caride AJ. 2007. Plasma-membrane $Ca^{2+}$ pumps: structural diversity as the basis for functional versatility. Biochem Soc Trans. 35:919–922.

Strehler EE, Zacharias DA. 2001. Role of alternative splicing in generating isoform diversity among plasma membrane calcium pumps. Physiol Rev. 81:21–50.

Strotmann J, Levai O, Fleischer J, Schwarzenbacher K, Breer H. 2004. Olfactory receptor proteins in axonal processes of chemosensory neurons. J Neurosci. 24:7754–7761.

Weeraratne SD, Valentine M, Cusick M, Delay R, Van Houten JL. 2006. Plasma membrane calcium pumps in mouse olfactory sensory neurons. Chem Senses. 31:725–730.

Zhang W, Delay RJ. 2006. Pulse stimulation with odors or IBMX/forskolin potentiates responses in isolated olfactory neurons. Chem Senses. 31: 197–206.

Zimmerman AL. 2006. The sweet smell of success: conclusive evidence that cyclic AMP hydrolysis does not trigger fast adaptation in olfactory receptor cells. J Gen Physiol. 128:149–151.

*Accepted February 15, 2009*